



THE UNIVERSITY *of* EDINBURGH

## Edinburgh Research Explorer

# Metabolic control analysis for drug target selection against human diseases

### Citation for published version:

Belmont-Díaz, J, Vázquez, C, Encalada, R, Moreno-Sánchez, R, Michels, P & Saavedra, E 2022, Metabolic control analysis for drug target selection against human diseases. in MT Scotti & CL Bellera (eds), *Drug target identification and validation*. Computer-aided drug discovery and design, vol. 1, Springer Nature Switzerland AG, pp. 201-226.

### Link:

[Link to publication record in Edinburgh Research Explorer](#)

### Document Version:

Peer reviewed version

### Published In:

Drug target identification and validation

### General rights

Copyright for the publications made accessible via the Edinburgh Research Explorer is retained by the author(s) and / or other copyright owners and it is a condition of accessing these publications that users recognise and abide by the legal requirements associated with these rights.

### Take down policy

The University of Edinburgh has made every reasonable effort to ensure that Edinburgh Research Explorer content complies with UK legislation. If you believe that the public display of this file breaches copyright please contact [openaccess@ed.ac.uk](mailto:openaccess@ed.ac.uk) providing details, and we will remove access to the work immediately and investigate your claim.



## **Metabolic Control Analysis for drug target selection against human diseases**

Javier Belmont-Díaz<sup>1</sup>, Citlali Vázquez<sup>1</sup>, Rusely Encalada<sup>1</sup>, Rafael Moreno-Sánchez<sup>1</sup>, Paul A. M. Michels<sup>2\*</sup>, Emma Saavedra<sup>1\*</sup>

<sup>1</sup> Departamento de Bioquímica, Instituto Nacional de Cardiología Ignacio Chávez. Mexico City, Mexico.

<sup>2</sup> Centre for Immunity, Infection and Evolution (CIIE) and Centre for Translational and Chemical Biology (CTCB), School of Biological Sciences, The University of Edinburgh, Edinburgh, Scotland.

\* Corresponding authors

Emma Saavedra, Ph.D.

Departamento de Bioquímica, Instituto Nacional de Cardiología Ignacio Chávez. Juan Badiano N° 1 Col. Sección XVI, Tlalpan, Mexico City, 14080, Mexico  
Tel. (+5255) 5573-2911 ext. 25501.

e-mail: emma\_saavedra2002@yahoo.com

Paul A.M. Michels, Ph.D.

School of Biological Sciences, The University of Edinburgh, The King's Buildings, Charlotte Auerbach Road, Edinburgh EH9 3FL, Scotland  
Tel.: +44-131-6505750

e-mail: paul.michels@ed.ac.uk

Running title: Metabolic Control Analysis for drug target validation

## Abstract

For identification of suitable therapeutic targets (enzymes/transporters) in intermediary metabolism of pathological and parasitic cells, the capacity of the target to govern the metabolic pathway flux should be considered. Metabolic Control Analysis (MCA) is a biochemical framework that enables to quantitate the degree of control that the activity of a target  $i$  ( $a_i$ ) exerts on the pathway flux ( $J$ ), defined as flux control coefficient ( $C_{a_i}^J$ ). Different experimental strategies are being used to determine the  $C_{a_i}^J$  of individual pathway steps, and consequently, the distribution of control in the metabolic pathway. By applying MCA, the components with the highest control on flux can be identified, which are the targets with the highest therapeutic potential. In this chapter we will review the MCA theoretical principles and experimental approaches to determine the  $C_{a_i}^J$  in a range of metabolic pathways such as central carbon and antioxidant metabolism, with potential application to other pathways of diverse human diseases.

Key words: Drug target, Metabolic Control Analysis, flux control coefficient, intermediary metabolism, pathway modeling.

## 1. Introduction

Targeting of metabolic pathways has emerged as an alternative approach with potential for drug discovery in order to find novel therapeutic strategies against a diversity of human diseases such as parasitic ones (Mukherjee et al 2016; Muller and Hemphill, 2016; de Rycker et al 2018; Raj et al 2020; Tyagi et al 2019), immune disorders (Castegna et al 2020), and cancer (Galluzzi et al 2013; Moreno-Sánchez et al 2010; 2014; Kaambre et al 2013). Identification of suitable metabolic targets among the multitude of enzymes and transporters that constitute the cell metabolic networks, although an apparently simple task, it is a very challenging endeavor.

In general, the most divergent enzymes of intermediary metabolism between normal *versus* parasitic or pathological cells have been proposed as drug targets. For instance, pathway enzymes that are only present in parasites or that significantly diverge from those in the human cells. Specific examples are some enzymes of glycolysis (Muller et al 2012; Saavedra et al 2019; Michels et al 2021), the antioxidant defense in trypanosomatids (Saavedra et al 2019; Talevi et al 2019) or nucleotide synthesis (Valente et al 2019). For human diseases with the highest death tolls such as cancer, identification of drug targets becomes even more difficult due to the similarity of the enzymes in the normal *versus* pathological cells. Thus, differences in enzyme expression levels, isoform expression, and pathway regulation have been used to propose novel metabolic candidates for drug targeting (Marin-Hernandez et al 2009; 2014; Sukjoi et al 2021).

Experimental strategies involving gene knockout or knockdown and more recently gene editing through CRISPR-CAS and RNAi libraries have been used to identify drug targets (reviewed in Wyatt et al 2011; Soares-Medeiros et al 2017; de Rycker et al 2018; Kurata et al 2018; Schuster et al 2019). In general, these strategies drastically lower the level of a protein, leading to the conclusion that the intervened gene is essential for cell survival or for a specific physiological function and therefore the gene product becomes validated as a suitable drug target. However, such large decreases in the content and activity

of the targeted protein can be far from being achieved by pharmacological methods.

For these reasons, it seems required to include additional criteria to narrow the drug target options and identify the most convenient targets before embarking on a process of drug design or to screen a library of compounds. It is in this context that Metabolic Control Analysis (MCA), a biochemical framework to analyze the control of metabolism quantitatively, can be a valuable tool to refine drug target selection with the aim to improve existing therapeutic strategies.

## 2. Basic principles of Metabolic Control Analysis

A criterion for drug target selection in the intermediary metabolism networks can be based on the capacity that the target (enzyme or transporter) has to influence the flux of the metabolic pathway of interest. A quantitative form to assess it is through the MCA fundamentals (Fell 1997; Nelson and Cox 2017; Moreno-Sánchez et al 2008b; Saavedra et al 2019). MCA was developed independently by two groups, Kacser and Burns in Edinburgh, Scotland (Kacser and Burns, 1973), and Heinrich and Rapoport in Berlin, Germany (Heinrich and Rapoport, 1974). MCA is a theoretical framework that considers metabolic processes as a continuous flow in steady state of matter and energy, in which each component of the metabolic pathway exerts some *control* over the pathway flux (Fell, 1997; Nelson and Cox 2017).

Here it is necessary to distinguish the concepts of *control* and *regulation*, frequently found in biochemistry textbooks and the scientific literature as interchangeable, but that in MCA, like in engineering, have very different meanings. **Regulation** refers to the molecular mechanisms by which a cell maintains its homeostasis, (*i.e.* to maintain a physiological variable at constant level), to be able to change to a new metabolic status when it is exposed to a different environmental condition. Within these mechanisms are those of protein covalent modification, compartmentalization, protein synthesis and degradation and allostereism that can modify the activity of a preexisting

enzyme; or transcriptional regulation to up or down regulate the expression of specific enzymes (Newsholme and Start, 1973).

In contrast, **Control** is the capacity of an enzyme, transporter or physiological process to affect the pathway flux under a defined metabolic steady state (Fell, 1997; Nelson and Cox, 2017; Moreno-Sánchez et al 2008b, Saavedra et al 2019). To illustrate this, ATP phosphofructokinase (PFK I) and pyruvate kinase (PyK) are highly *regulated* glycolytic enzymes able to drastically change the metabolic fluxes in different metabolic states to avoid futile cycles, e.g. during feed and starvation, which concur with changes of high and low blood glucose concentrations and thus with glycolysis and gluconeogenesis activation, respectively. Once a new stable metabolic steady state is reached, these enzymes do not necessarily exert significant *control* on the pathway flux any longer. As discussed below, glucose transport has significant control on stable steady state glycolysis fluxes of several cell models, whereas PFK-1 and PyK have low or negligible control (reviewed in Moreno-Sánchez et al 2008b; Saavedra et al 2019).

MCA is based on the following basic considerations:

- 1) The metabolic pathway must be at a stable steady state or quasi steady state. In order to achieve that condition, the system must be open and the initial substrates and final products have to be kept at constant levels.
- 2) At steady state, the rate ( $v$ ) of each pathway component (enzyme, transporter) in a linear metabolic pathway is the same, and it is similar to the rate or production of the pathway's end product. Usually the rate of the pathway enzymes under metabolic steady state is lower than their maximal activities ( $V_{max}$ ); hence, commonly there is a generalized excess of enzyme activity capacity in comparison to the pathway flux values.
- 3) Proper stoichiometric relationships of the pathway's substrates and end products have to be considered for the analysis of flux control distribution. This is, for example, relevant in branched pathways where unequal input and output of metabolic intermediates may occur.
- 4) Parameters are quantities that can be changed independently, and they typically remain constant during the evolution of the system toward its steady state, for example, kinetic constants, enzyme activity ( $V_{max}$ ).

5) Variables are quantities determined by the system, and they are time-dependent before reaching a given steady state. Variables are, for example, metabolic flux, metabolite concentration, enzyme or transport rates ( $v$ ) or rates of any other physiological process (pathway branches).

To determine the degree of influence that a perturbation in a parameter (e.g. enzyme activity) has over a pathway variable at steady-state (e.g. pathway flux), the MCA theory relies on three types of coefficients (control, elasticity and response) and two theorems that relate them (summation and connectivity). These constitute the fundamentals of MCA.

## 2.1. Control coefficients

The control coefficient quantifies the impact that a perturbation in the activity of an enzyme has on the pathway steady-state response, either on its flux (flux control coefficient) or on the concentration of a pathway intermediate metabolite (concentration control coefficient).

The flux control coefficient quantifies how much the pathway flux changes when the activity of an enzyme is changed; this coefficient is mathematically represented as:

$$C_{a_i}^J = \frac{\delta J}{\delta a_i} \left( \frac{a_{i0}}{J_0} \right) \dots \dots (Eq 1)$$

where  $J$  is the pathway flux at steady state and  $a_i$  is the activity  $a$  of enzyme  $i$ . By multiplying by the scalar factor  $a_{i0}/J_0$  which corresponds to the ratio of the enzyme activity and pathway flux in the unperturbed (control) state, the  $C_{a_i}^J$  becomes dimensionless and independent of the units used.

On the other hand, the concentration control coefficient quantifies how much the concentration of a pathway intermediate metabolite changes when the activity of an enzyme is changed, and this coefficient is mathematically defined by:

$$C_{a_i}^X = \frac{\delta X}{\delta a_i} \left( \frac{a_{i0}}{X_0} \right) \dots \dots (Eq 2)$$

where  $X$  and  $X_0$  are any pathway intermediate metabolite in the perturbed and unperturbed states, respectively.

From here, the chapter will be focus on the experimental assessment and analysis of the flux control coefficients because it concerns to drug target validation. For further information on concentration control coefficients and their theorems, which are relevant for biotechnological purposes, the reader is referred to the book by Fell (1997).

## 2.2. Summation theorem

Kacser and Burns (1979) demonstrated that, regardless of the complexity of the kinetic mechanisms governing each enzymatic (and transport) component from a metabolic pathway, the sum of their control coefficients equals to unity. This relationship is named as the summation theorem and is expressed in equation 3 for pathway flux:

$$\sum_{i=1}^n C_{a_i}^J = 1 \dots \dots (Eq 3)$$

This summation theorem reveals some important properties of  $C_{a_i}^J$  listed below:

- If one enzyme activity is changed by a substantial amount, its  $C_{a_i}^J$  is changed to a new value and the  $C_{a_i}^J$  of all other enzymes must have changed, so that the new sum, again, equals 1.
- Some of the individual  $C_{a_i}^J$  will be “negligibly small”, however the sum of these “small”  $C_{a_i}^J$  may not be negligible.
- The larger the number of enzymes included in the pathway, the smaller the average  $C_{a_i}^J$  for all enzymes.
- Typical values of  $C_{a_i}^J$  are between 0 and 1 ( $0 < C_{a_i}^J < 1$ ). However, the  $C_{a_i}^J$  are negative for enzymes that branch off from the main pathway and



withdraw metabolites, whereas the  $C_{ai}^J$  will be positive for branches that supply intermediates to the main pathway.

### 2.3 Flux control coefficient estimation

In theory,  $C_{ai}^J$  can be determined by measuring the infinitesimal changes of the flux at steady state induced by an infinitesimal change in the activity of an enzyme. Thus, the  $C_{ai}^J$  can be estimated from the slope of the tangent line to the activity of the enzyme in the unperturbed steady state of interest (the basal value of activity or 100% activity). By analyzing the enzyme behavior shown in Figure 1, it is clear that inhibition of the activity of an enzyme with a  $C_{ai}^J = 0.5$  (panel A) induces larger decreases in flux than inhibition of an other one with  $C_{ai}^J = 0.1$  (panel B). Furthermore, 50% inhibition of the activity of enzyme of panel A will lead almost to total control on the pathway flux ( $C_{ai}^J$  from 0.5 to 0.7), whereas the same inhibition of the enzyme in panel B will gain control, but still not meaningful ( $C_{ai}^J$  from 0.1 to 0.2). Hence, it becomes evident that the best therapeutic targets are enzymes or transporters that have a high  $C_{ai}^J$  ( $> 0.5$ ) under physiological conditions.

Figure 1 also shows that at enzyme activity inhibitions  $> 90\%$  (orange lines) there is no difference on the pathway flux reduction amongst high and low flux controlling enzymes, both reaching similar  $C_{ai}^J$  of 0.9. It should be realized that it is in that range of decreased expression and activity that drug targets are validated as essential by genetic methods.

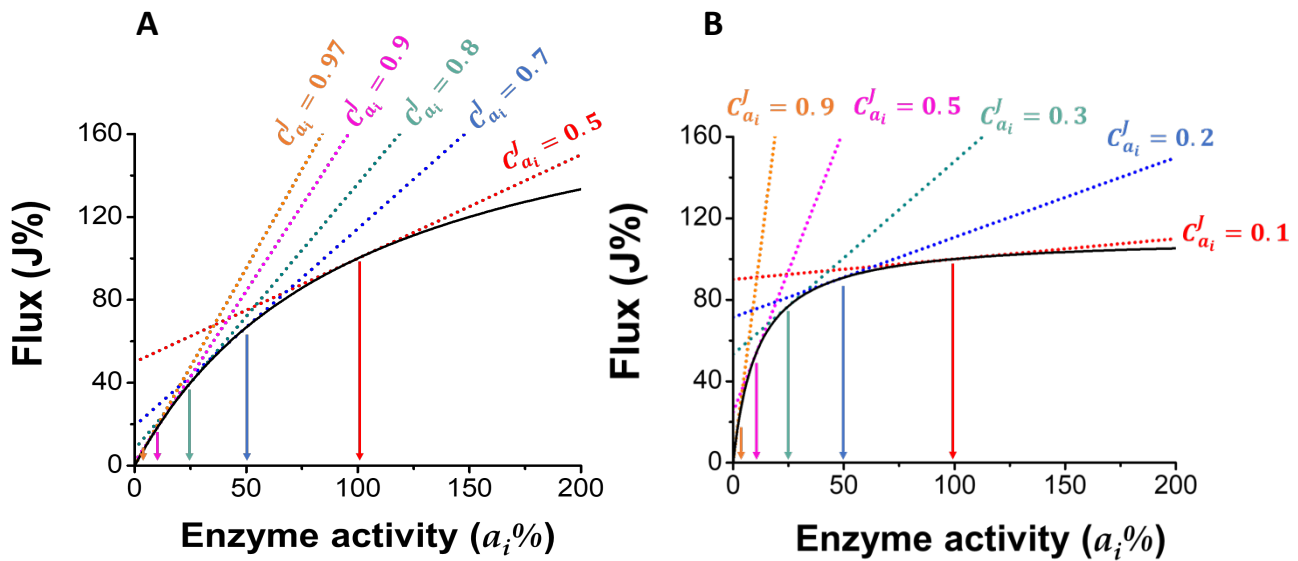


**Figure 1. Direct experimental determination of the flux control coefficient ( $C^J_{a_i}$ )**

**A)** The plot represents an enzyme that has a  $C^J_{a_i}=0.5$  at physiological conditions (100% of enzyme activity and 100% of flux). As the activity of the enzyme is slightly inhibited, it gains significant control on the pathway flux. **B)** The plot represents an enzyme with a  $C^J_{a_i}=0.1$  at physiological conditions. The same inhibition percentages as used in panel A were used for this model and the respective  $C^J_{a_i}$  is presented for each condition. For this low controlling enzyme to gain a control of 0.5 over the pathway flux, its inhibition must be greater than 90% (pink dot line). The plot was obtained by simulations using equation 9 considering  $n=1$ ,  $J_i=0$  and a  $C^J_{a_i}= 0.5$  or  $0.1$ , and the software Microcal Origin v. 8.0. The straight dotted lines are the derivatives at the point indicated by the arrows.

In practice, experimental approaches using genetic engineering commonly induce large changes in both enzyme activity and pathway flux (Fell 1997) to visualize “phenotype changes”. To circumvent this problem, a theoretical framework was created that allows accurate estimation of the control coefficients from the experimental data (Small and Kacser 1993a, b). In accordance with this theoretical framework, the  $C_{a_i}^J$  in a system with large changes of enzyme activity in a linear metabolic pathway is defined as follows:

$$C_{a_{i0}}^{J_0} = \frac{\Delta J/J_r}{\Delta a_i/a_{ir}} \dots \dots (Eq 4)$$

where  $\Delta J$  is the change of the flux from the original steady state ( $J_0$ ) to the resulting one after the enzyme activity has changed by a factor  $r$  ( $J_r$ ). Hence  $\Delta J = J_r - J_0$ , and  $\Delta a_i$  is the change of the enzyme activity from the original state ( $a_{i0}$ ) to the new enzyme activity ( $a_{ir} = r \cdot a_{i0}$ ), hence ( $\Delta a_i = a_{ir} - a_{i0}$ ) (Fell 1997; Small and Kacser 1993a). Rearranging equation 4, we have the following:

$$C_{a_{i0}}^{J_0} = \frac{(J_r - J_0)/J_r}{(ra_{i0} - a_{i0})/ra_{i0}} = \frac{1 - (J_0/J_r)}{(r - 1)/r} \dots \dots (Eq 5)$$

defining the amplification factor ( $f$ ) as the ratio of the new flux ( $J_r$ ) to the original one ( $J_0$ ) ( $f = J_r/J_0$ ) and rearranging equation 5, we obtain:

$$f = \frac{1}{1 - \frac{r-1}{r} C_{a_i}^J} \dots \dots (Eq 6)$$

This last function shows that by increasing the activity of a single enzyme, the effect on the pathway flux will be low when its  $C_{a_i}^J$  is below 0.5 (Fig. 2) (Fell 1997). For example, if a 10-times increase ( $r=10$ ) of enzyme activity is attained, and the enzyme has a  $C_{a_i}^J = 0.2$ , then the flux only increases 25%. On the other hand, decrease of enzyme activity (e.g., by a drug) always leads to a drop in the pathway flux which depends on the enzyme's  $C_{a_i}^J$ . For

example, a 10-times inhibition ( $r=0.1$ ) of an enzyme with  $C_{ai}^J = 0.2$ , induces a 65% decrease of the pathway flux, but lower inhibition levels do not relevantly affect the flux. The most interesting drug targets are enzymes with  $C_{ai}^J$  higher than 0.5, that require less inhibition degrees ( $r=0.5$ ) to observe flux inhibition.

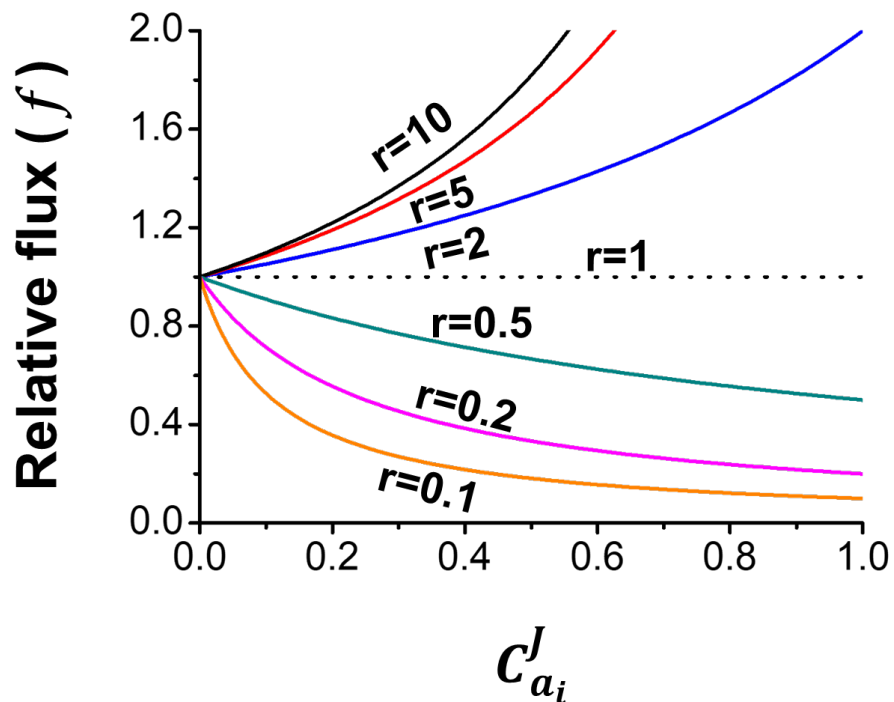


**Figure 2. Relative change of flux ( $f$ ) for large changes in enzyme activity in a linear pathway**

The plot was obtained by simulations with equation 6 using the software Microcal Origin v. 8.0. The degree of amplification,  $r$ , meaning overexpression or genetic down-regulation is shown at each curve.

### 2.3.1 Relationship between flux and enzyme activity

There is no way to predict the behavior of the flux of a metabolic pathway as a function of a unique enzyme activity and therefore it is not possible to propose a general equation that describes this behavior. However, it has been empirically observed that the pathway flux shows a hyperbolic behavior as a function of the activity of the pathway enzymes, especially when the pathway is *in vitro* reconstituted (Gellerich et al 1990; Fell 1997; González-Chávez et al 2015 and 2019). Therefore, the following equation has been proposed (Gellerich et al 1990):

$$J = \frac{\alpha a_i}{\beta + a_i} \dots \dots (Eq 7)$$

where  $\alpha$  and  $\beta$  are empiric constants. In a more general way, equation 7 can be rewritten as follows:

$$J = \frac{\alpha a_i^n}{\beta + a_i^n} + J_i \dots \dots (Eq 8)$$

where  $J_i$  represents an initial flux that persists even when the activity of the enzyme ( $a_i$ ) is zero and “ $n$ ” is an empirical constant which gives a sigmoidal behavior (Gellerich et al 1990). A more useful form of equation 8 is obtained when the constants  $\alpha$  and  $\beta$  are expressed in terms of the control coefficient at the basal condition of 100% of flux and 100% of enzyme activity (Eq. 9) (Gellerich et al 1990; Rodríguez-Enríquez et al 2000):

$$J = \frac{n (100 - J_i)^2 a_i^n}{100^{n+1} C_{a_{i0}}^{J_0} + [n(100 - J_i) - 100 C_{a_{i0}}^{J_0}] a_i^n} \dots \dots (Eq 9)$$

The relationship between the flux and the enzyme activity expressed in Eq. 9 is graphically represented in Fig. 3. Again, almost linear decreases in flux are attained by inhibition of enzymes with  $C_{ai}^J$  greater than 0.5.

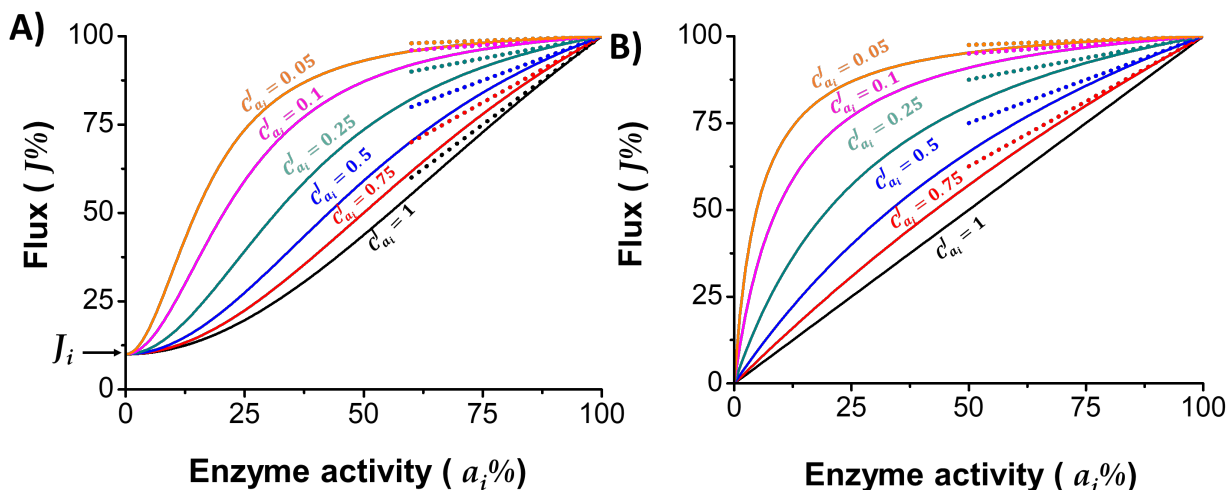


**Figure 3. Theoretical relationship between enzyme activity and flux.**

A) The plot represents a case when the relationship between enzyme activity and flux is sigmoidal ( $n > 1$  in Eq. 9) and a residual flux is obtained despite a null activity ( $J_i$ ). For illustrative purpose, we use a model with  $n=2$  and  $J_i=10$ . B) The plot represents the most used fitting model where the relationship between activity and flux is hyperbolic ( $n=1$ ,  $J_i=0$ ). Both plots were obtained from simulations using equation 9 and the software Microcal Origin v. 8.0. The values of control coefficients ( $C_{ai}^J$ ) are those of the slope of the tangent line at the basal condition of 100% of pathway flux and 100% of enzyme activity (marked with the dotted line).

## 2.4 Experimental determination of the control coefficient

In order to experimentally determine the  $C_{ai}^J$  it is necessary to modify the activity of a single enzyme at a time (without affecting the rest of the pathway enzymes), while determining the metabolic pathway flux. To achieve such condition, several experimental strategies have been successfully carried out: enzyme titrations with specific inhibitors, *in vitro* reconstitution of the pathway or pathway segments and genetic manipulation of enzyme expression in cells.

### 2.4.1 Enzyme titration with inhibitors

Titration of enzyme activity by using inhibitors to estimate control coefficients is restricted by the degree of specificity that inhibitors have. The availability of specific, potent and permeable mitochondrial inhibitors has made it possible to use this approach to determine the  $C_{ai}^J$  of several complexes and enzymes of oxidative phosphorylation (OxPhos) in diverse organs. When the flux of ATP synthesis is titrated by adding increasing concentrations of each specific inhibitor, plots are generated in which the enzyme activity is progressively diminished at increasing inhibitor concentration (Moreno-Sánchez 2008b) and the  $C_{ai}^J$  can be estimated from the initial slope (graphical determination).

However, the titration curves are in general sigmoidal, complicating the calculus of the initial slope by graphical determination, which can lead to overestimation of  $C_{ai}^J$  values (Gellerich et al 1990). For this reason, equations for non-linear curve fitting have been developed depending on the type of inhibitor used (Moreno-Sánchez 2008b). The values of  $C_{ai}^J$  estimated for OxPhos depend on experimental conditions (*e.g.*, whole cells, isolated mitochondria), the tissue and the equation used for each inhibitor. These considerations have been appropriately reviewed previously (Moreno-Sánchez 2008b).

Two examples that use a variation of equation 9 are discussed below. Antimycin A (inhibitor of cytochrome bc1 in complex III) and carboxyatractyloside (inhibitor of the adenine nucleotide translocator) are tightly-bound inhibitors that were used to estimate  $C_{ai}^J$  over total mitochondrial

respiration in isolated rat liver mitochondria (Gellerich et al 1990). The non-linear curve fitting of titrations with these inhibitors allowed to determine the inhibitor affinity constants,  $K_d = 7.8$  pM and  $K_d = 0.86$  nM for antimycin A and carboxyatractyloside, respectively. The estimated  $C_{ai}^J$  was 0.2 for complex III and 0.34 for the adenine nucleotide translocator.

The same experimental approach and equation were used to determine the  $C_{ai}^J$  of mitochondrial components in OxPhos of hepatoma cells (Rodríguez-Enríquez et al 2000). Specific mitochondrial inhibitors were used to estimate the  $C_{ai}^J$  of NADH dehydrogenase inhibited by rotenone ( $C_{ai}^J=0.3$ ), bc1 cytochrome complex inhibited by antimycin A ( $C_{ai}^J=0.23$ ), cytochrome c oxidase inhibited by cyanide ( $C_{ai}^J=0.04$ ), ATP synthase inhibited by oligomycin ( $C_{ai}^J=0.02$ ), ATP/ADP translocase inhibited by carboxyatractyloside ( $C_{ai}^J=0.3$ ) and pyruvate carrier inhibited by 3-hydroxycinnamate ( $C_{ai}^J=0.026$ ). Thus, control of OxPhos relied mainly on three reactions. Applying the summation theorem (Eq. 3) to this example, the processes studied control about 0.92 of OxPhos, so all other reactions involved in OxPhos are responsible for the remaining 0.08; hence the transport of substrates (pyruvate or phosphate carriers), dehydrogenases (succinate dehydrogenase) and ATP synthase, exert negligible control over the OxPhos flux.

#### 2.4.2 *In vitro* pathway reconstitution

This approach is based on the *in vitro* reconstitution of segments of the metabolic pathway using purified enzymes. The *in vitro* pathway reconstitution must simulate as much and close as possible the *in vivo* conditions of the pathway. This should be carried out regarding (1) the ratio of enzyme activities present in the model under study, for which their actual  $V_{max}$  values within the cell have to be determined at the physiological intracellular high  $K^+$  medium, pH and growth temperature of the biological model used; and (2) the physiological concentrations of substrates and coenzymes.

The titration curve of enzyme activity *versus* pathway flux (Fig. 1) has to be constructed by varying the activity of one enzyme at a time while keeping the rest of the system (partner enzymes, substrates, and cofactors) unaltered and in



parallel determining changes in the pathway flux. A limitation of these *ex vivo* experiments is that only a quasi-steady state is attained because there is net substrate consumption and product accumulation. However, by using short times of the reaction system and adding saturating substrate concentrations these problems can be circumvented.

This strategy was first applied for segments of glycolysis using mammalian enzymes due to the availability of commercial proteins or methods for their purification. Torres et al (1986; 1989) used pure enzymes added to cell extracts or in a cell free system, respectively, to determine the  $C^J_{ai}$  for the first glycolytic segment, finding that hexokinase (HK) and PFK-1 have the highest  $C^J_{ai}$ . In these studies the summation theorem was demonstrated. On the other hand, Giersch (1995) reconstituted the final pathway segment of glycolysis with commercial pure enzymes, where PyK was the controlling enzyme.

More recently, pathway reconstitution was performed for the pyrophosphate-dependent glycolysis of the intestinal parasitic protist *Entamoeba histolytica*, which does not have the typical ATP dependent PFK-1 but an inorganic pyrophosphate-dependent enzyme (PPi-PFK) and, instead of PyK, a PPi-dependent pyruvate phosphate dikinase (PPDK). Both PPi-dependent enzymes catalyze reversible reactions which lead to a different type of metabolic regulation of this pathway (Pineda et al 2015a; Saavedra et al 2019). Pathway reconstitution was carried out using recombinant purified *E. histolytica* enzymes of the segments of HK to triosephosphate isomerase and from phosphoglycerate mutase (PGAM) to PPDK. It was found that HK and PGAM have the highest control of flux, with low control exerted by the PPi-dependent enzymes, indicating that despite their large structural divergence to the human enzymes, they are no suitable drug targets from the metabolic point of view (Moreno-Sánchez et al 2008a). In addition, the dataset of the amoebal pathway reconstitutions were also used for kinetic pathway modeling, which helped to unveil previously unknown inhibition of pathway intermediates on the glycolytic enzymes (Moreno-Sánchez et al 2008a) and also to improve other forms of pathway modeling by artificial neural networks (Lo-Thong et al 2020).

Pathway reconstitution was also applied to the trypanothione-dependent peroxide detoxification system of *Trypanosoma cruzi*, the parasitic protist that is responsible for Chagas disease in Latin America and for which no adequate

drugs are yet available. Trypanothione replaces glutathione as the main antioxidant system in the parasite and its entire peroxide detoxification machinery uses this metabolite as reductant (Fig. 4A). For several decades, this pathway has attracted attention for therapeutic intervention against the parasitic disease (Olin-Sandoval et al 2010; Leroux and Krauth-Siegel 2016; Manta et al 2018; Saavedra et al 2019; Talevi et al 2019; Pineyro et al 2021). For pathway reconstitution, the recombinant enzymes trypanothione reductase (TryR), tryparedoxin (TXN) and tryparedoxin peroxidase (TXNPx) were used (González-Chávez et al 2015; González-Chávez et al 2020) (Fig. 4A). In these studies a low control by TryR (a popular target for therapeutic intervention against trypanosomatids) was determined, while TXN and TXNPx have both a  $C_{ai}^J$  of 1, therefore together producing a value of 2, in apparent conflict with the summation theorem. However, this difference is caused by the involvement of TXN and TXNPx in two processes, reduction and oxidation (González-Chávez et al 2015), which contrasts with the situation for glycolytic enzymes in which each enzyme is involved in only one C-metabolite transformation.

### 2.4.3 Manipulation of enzyme expression in cells

Manipulation of enzyme expression in cells by genetic engineering is a very useful tool for direct estimation of control coefficients (González-Chávez et al 2020), since in principle, just one enzyme is modified at the time. However, it is important to determine the actual level of enzyme activity (not just protein level resulting from altered gene expression). Furthermore, it is mandatory to determine the activity of the other enzymes that participate in the pathway to ascertain that they are not changed by undesirable or pleiotropic effects by the genetic modification of the single, targeted enzyme. Pleiotropic effects are the main limitations of the strategy since cells are open systems and can have responses to the genetic modification beyond the control of the experimenter; thus, a detailed biochemical characterization of each clone of cells expressing different levels of each pathway enzyme has to be performed for proper MCA application.

One of the first studies where this strategy was applied using traditional genetics was done for the arginine pathway in the fungus *Neurospora crassa* (Flint et al 1981), where argininosuccinate synthetase was found to be the main controlling enzyme. For additional examples about other metabolic routes in different cell systems refer to Moreno-Sánchez et al (2008b). Downregulation by RNAi of the activities of HK, PFK, PyK, PGAM and enolase was performed in the glycolytic pathway of *Trypanosoma brucei*, the parasite responsible for sleeping sickness in sub-Saharan Africa. The study revealed that the first three enzymes have low flux control due to their overcapacity, as was also predicted by kinetic modeling (Albert et al 2005). In fact, the glucose transporter accounted for 40% of the flux control.

Modulation of protein expression was recently applied in the trypanothione synthesis and trypanothione-dependent antioxidant system of *T. cruzi* (González-Chávez et al 2019), where the expression of TryR and TXN of the peroxide detoxification system was modulated as well as that of two enzymes of the trypanothione synthesis pathway:  $\gamma$ -glutamylcysteine synthetase ( $\gamma$ ECS) and trypanothione synthetase (TryS) (Fig. 4A). It was demonstrated that  $\gamma$ ECS has a  $C_{ai}^J$  of 0.69 in the trypanothione synthesis flux (Fig. 4B), while TryS has at most a  $C_{ai}^J$  of 0.3. Furthermore, for the peroxide detoxification flux, TryR showed again a low  $C_{ai}^J$  of 0.15 (Fig. 4C), whereas TXN showed the highest  $C_{ai}^J$  of 0.73 (Fig. 4D). The latter two  $C_{ai}^J$  values were in agreement to those found by pathway reconstitution (see above, section 2.4.2) and by kinetic modeling as described later (section 4).

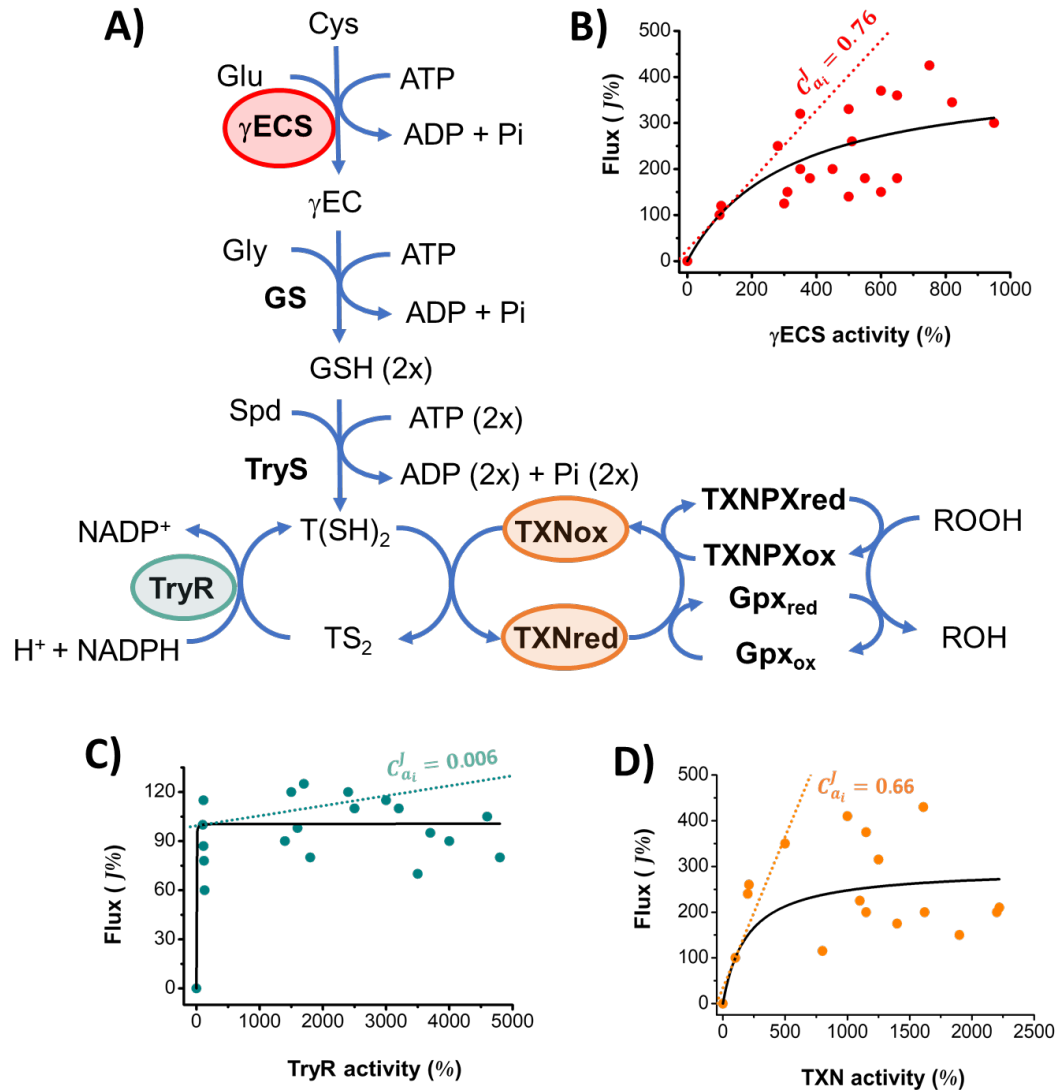


**Figure 4. Estimation of the control coefficient by enzyme overexpression**  
A) *Trypanosoma cruzi* antioxidant pathway, the overexpressed proteins were  $\gamma$ -glutamylcysteine synthetase ( $\gamma$ ECS), trypanothione reductase (TryR) and tryparedoxin (TXN). For experimental determination of  $C_{ai}^J$ , overexpressing clones with different levels of activity (low, medium, and high) were used and their effect on pathway fluxes was evaluated for B)  $\gamma$ ECS activity and its effect on  $T(SH)_2$  synthesis; C) TryR and D) TXN activities and their effect on the hydroperoxide reduction flux. Dotted lines are the tangent to the 100% values (WT condition). Data from panels B, C and D were taken from González-Chávez et al (2019) and fitted to equation 9 ( $n=1$ ). The estimated  $C_{ai}^J$  with the non-linear curve fit (using Microcal Origin v. 8.0) were consistent with values previously reported (Olin-Sandoval et al. 2012; González-Chávez et al 2019).

### 3. Elasticity coefficients

The flux in a metabolic pathway is the result of the concerted reaction rates of all components that constitute the metabolic pathway. Since the partial rate ( $v$ ) of each individual pathway component is the same in a linear metabolic pathway under steady-state conditions, it can be assumed that the rates of all the individual components are similar to the rate of production of the pathway's end product (pathway flux).

On the other hand, every enzyme within the pathway is connected to its upstream and downstream "neighbor" enzymes through its substrates and products. Further, it can be connected with "distant" enzymes or cellular processes through metabolic effectors such as inhibitors and activators produced by enzymes within the same pathway or from different pathways.

Theoretically, a perturbation in the activity of any given enzyme in the pathway could affect the rate of reaction of the other pathway enzymes. The transmission and amplification of this change will depend on the intrinsic properties of each enzyme (e.g., kinetic parameters) and on the concentration of the molecules participating in the enzyme-catalyzed reaction. The elasticity coefficient quantifies this transmission response (Kacser 1983).

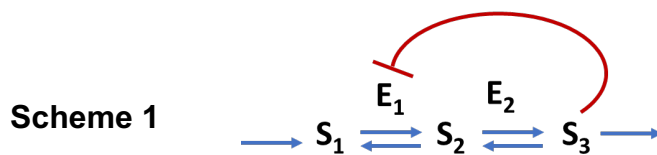
The elasticity coefficients are properties of the individual enzymes or transporters and quantify how much their rate is modulated by a variable (e.g., substrates, products, internal inhibitors/activators, pH, temperature) (Fell 1997; Brand 1998; Moreno-Sánchez et al 2008b; Saavedra et al 2019). The mathematical expression of the elasticity coefficient is:

$$\varepsilon_{X_{i0}}^{v_{i0}} = \frac{\partial v_i}{\partial X_i} \left( \frac{X_{i0}}{v_{i0}} \right) \dots \dots (Eq 10)$$

where  $v$  is the rate of a reaction (or transport) and  $X$  a **variable** that modifies the rate. Multiplication by  $X_{i0}/v_{i0}$ , which is the ligand concentration and rate in the unperturbed state, makes the coefficient dimensionless and thus independent of the units used.

The difference of the plots of enzyme rate *versus* substrate (or other ligand) concentration, typical of enzyme kinetic analyses using isolated enzymes, is that in the elasticity analysis the concentrations of ligands (pathway intermediates) are determined by the functioning of the entire metabolic pathway. Moreover, in the *in vitro* kinetic analysis of enzymes usually (1) only one ligand at a time is varied whereas the other co-substrates are kept constant; and (2) experiments are performed in the absence of products or inhibitors (“initial rate conditions”).

There are as many elasticity coefficients for each enzyme as there are substrates, products and effectors interacting with it. For example, the rate of enzyme 1 ( $v_1$ ) in scheme 1, depends on three variables, the concentration of  $S_1$ ,  $S_2$  and  $S_3$ .



Hence, the elasticity coefficients of scheme 1 for  $E_1$  are:

$$\varepsilon_{S_1}^{v_{E_1}} = \frac{\partial v_{E_1}}{\partial S_1} \left( \frac{S_1}{v_{E_1}} \right); \quad \varepsilon_{S_2}^{v_{E_1}} = \frac{\partial v_{E_1}}{\partial S_2} \left( \frac{S_2}{v_{E_1}} \right); \quad \varepsilon_{S_3}^{v_{E_1}} = \frac{\partial v_{E_1}}{\partial S_3} \left( \frac{S_3}{v_{E_1}} \right)$$

There are two ways to estimate the elasticity coefficient of a component from a metabolic pathway. (1) If the rate equation that describes the enzyme or transporter is known and it contains the variable to which the elasticity has to be calculated, the theoretical elasticity can be calculated from such equation; and (2) If the rate equation is not known, then the elasticity has to be experimentally estimated. These methods are described in the next section.

### 3.1 Estimation of the elasticity coefficient from the rate equation

The elasticities are intrinsically linked to the enzyme or transporter kinetics and can be calculated by solving the differential equation of the kinetic

rate expression with respect to the variable or parameter of interest and subsequently interpolating the value of the steady-state concentration of the variable of interest (Groen et al 1986; Fell, 1997; Moreno-Sánchez et al 2008b). For example, if the enzyme of interest follows reversible Michaelis-Menten kinetics, the expression of elasticity is:

$$\varepsilon_S^{v_{i0}} = \frac{\partial v_i}{\partial S} \left( \frac{S_0}{v_{i0}} \right) = \frac{1}{1 - \Gamma/Keq} - \frac{[S]/Ks}{1 + [S]/Ks + [P]/Kp} \dots \dots (Eq 11)$$

where the term  $\Gamma$  (gamma upper case) is the mass-action ratio which is defined as the ratio between the concentration of products and the concentration of substrates at steady state ( $\Gamma = [P]_{ss}/[S]_{ss}$ ).  $Keq$  is the equilibrium constant of the reaction ( $Keq = [P]_{eq}/[S]_{eq}$ ). When analyzing equation 11, it is evident that as the value of  $\Gamma$  gets closer to the equilibrium conditions ( $Keq$ ), then the elasticity value increases, and as the enzyme becomes more saturated with substrate ( $[S]/Ks$  increases), the value of elasticity decreases. This behavior is illustrated in Figure 5.

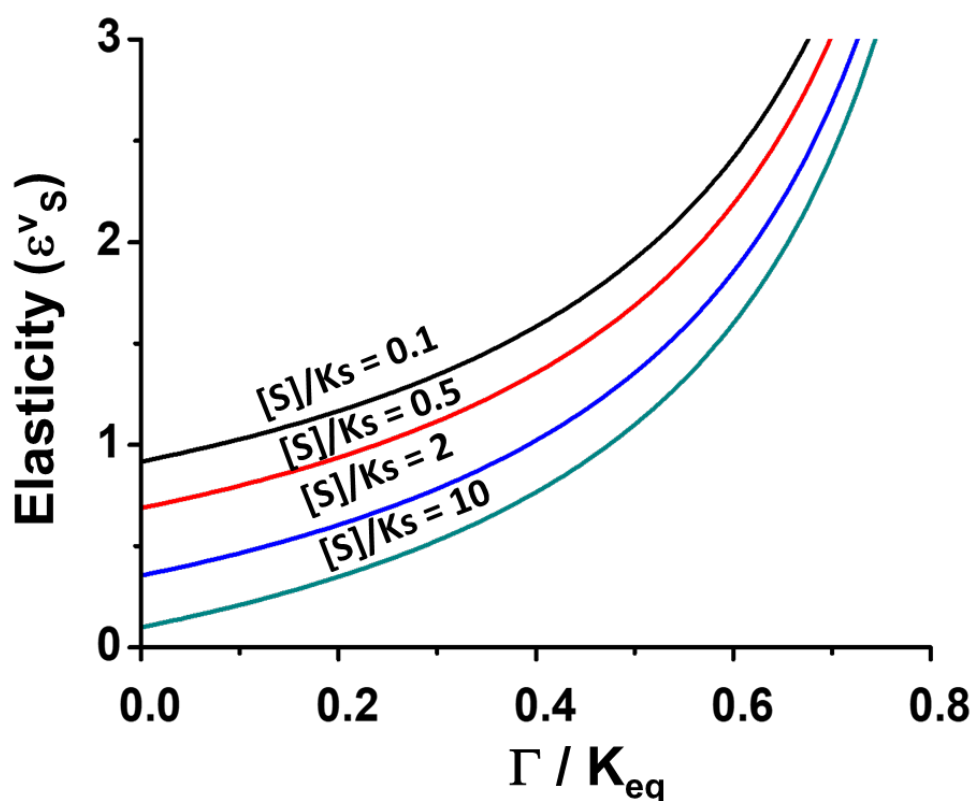


**Figure 5. Variation of elasticity with respect to the disequilibrium ratio ( $\Gamma/K_{eq}$ )**

The plot shows that the elasticity coefficient ( $\varepsilon^v_s$ ) of an enzyme increases as the value of the mass-action ratio ( $\Gamma$ ) approximates to the value of the equilibrium constant ( $K_{eq}$ ). In this plot it is also observed that when the saturation of the enzyme ( $[S]/K_s$ ) increases, the elasticity value decreases. The graph was obtained by simulations using equation 11 and the software Microcal Origin v. 8.0 ( $[P]/K_p = 0.1$  for all curves).



### 3.2 Estimation of the elasticity coefficient from the substrate saturation curves

Direct *in vitro* measurement of elasticities is in theory difficult to accomplish since only one modulator has to be varied and the other molecules that affect the enzyme activity have to be kept constant and under steady-state conditions. If these conditions are met, then the elasticity coefficient can be estimated from the slope of the tangent line to the concentration of the variable at the steady state of interest, which is at the steady-state concentration of ligands in the cell (Fig. 6). The elasticity coefficients are positive ( $\varepsilon^v_x > 0$ ) for those variables that increase the enzyme or transporter rate (substrate or activator), and they are negative ( $\varepsilon^v_x < 0$ ) for the variables or parameters that decrease the enzyme or transporter rates (product or inhibitor).

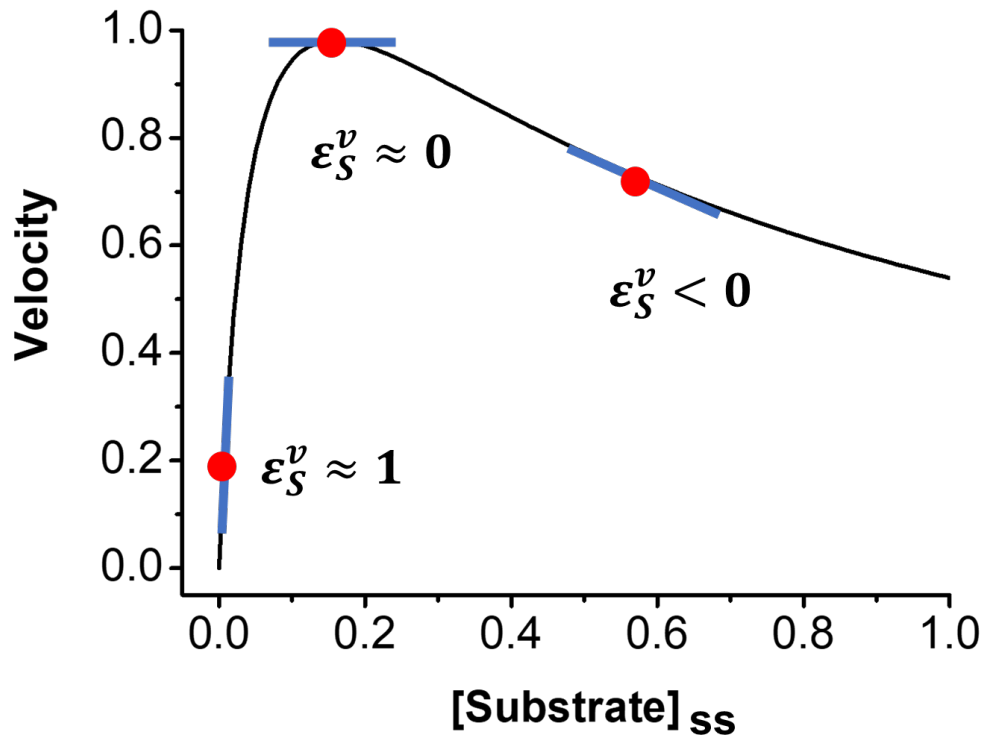


**Figure 6. Estimation of elasticity coefficients from the saturation curve**

The plot represents an enzyme with substrate inhibition ( $v = \frac{V_{max} [S]}{K_s(1+[S]/K_{is}) + [S](1+[S]/\alpha K_{is})}$ ). The elasticity coefficient of an enzyme towards a substrate (or any other ligand) is determined from the slope of the tangent line (or derivative) at the concentration of substrate at the control steady state. When the steady-state substrate concentration ( $[S]_{ss}$ ) is below the  $K_s$  (or  $K_m$ ) value, the  $\varepsilon_s^v \approx 1$ , which means that the enzyme is highly responsive to substrate variation. In contrast, if  $[S]_{ss}$  is near to saturation,  $\varepsilon_s^v \approx 0$ , which means that the enzyme is saturated and cannot vary its rate. Finally, if  $[S]_{ss}$  is in the zone of inhibition ( $[S] \geq \alpha K_{is}$ ), the elasticity will have negative values ( $\varepsilon_s^v < 0$ ).

### 3.3 Experimental determination of the elasticity coefficient within cells

Elasticity analysis can be experimentally determined using live intact cells (Fig. 7). Elasticity coefficients of an enzyme or groups of enzymes around a metabolite are determined by monitoring the changes in pathway flux in response to changes in the concentration of an intermediate metabolite. The changes in the metabolite concentration are performed by manipulating the rates of the group of enzymes that supply it by feeding the pathway with the pathway's initial substrate (Fig. 7A). For example, this can be done by providing increasing concentrations of glucose for glycolysis to the cells. In another set of experiments, the intermediary metabolite concentration is manipulated by inhibition of a reaction downstream of the metabolite of interest, for example inhibiting lactate dehydrogenase for glycolysis or E2 in Fig. 7A. From plots like those shown in Fig. 7B, the elasticity coefficients of the group of reactions that supply and demand a metabolite are determined. If similar experiments are carried out by monitoring different pathway intermediate metabolites, the elasticity coefficients of individual reactions can be determined and from these, the flux control coefficients calculated by the connectivity theorem as described next.

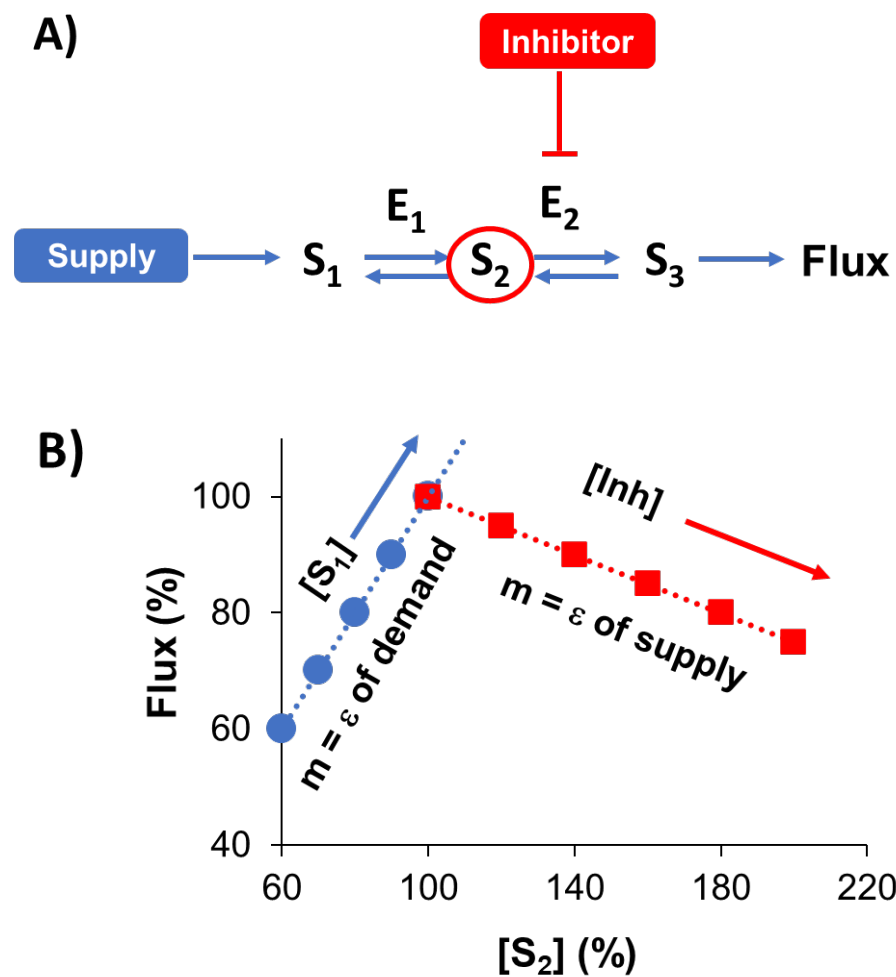


**Figure 7. Determination of the elasticity coefficient of one enzyme or group of enzymes of a metabolic pathway**

**A)** Scheme that represents manipulation of the pathway intermediate  $S_2$  to evaluate the elasticities of  $E_1$  (supply reactions) and  $E_2$  (demand reactions). Let us recall that, at steady state, the rate of reactions by these enzymes will be equal to the final flux in a linear metabolic pathway. In this example  $S_2$  is substrate of  $E_2$ , thus increases in  $S_2$  concentration attained by supplying  $E_1$  will increase the rate of  $E_2$ . On the other side,  $S_2$  is a product of  $E_1$ , thus increases in  $S_2$  concentration by  $E_2$  inhibition will promote rate inhibition of  $E_1$ . **B)** Plot of a theoretical behavior of the manipulation of a pathway intermediate  $S_2$  by increasing the concentration of a supply metabolite ( $S_1$ ) or by the inhibition of an enzyme in the pathway after  $S_2$ . The elasticity coefficient of  $E_2$  (or  $S_2$  demand) is calculated from the slope of the tangent line closest to 100% resulting from the increase in  $[S_1]$  concentration (blue dots). The elasticity coefficient of  $E_1$  (or  $S_2$  supply) is estimated from the slope of the tangent line to the curve closest to 100% resulting from the increase in  $[Inh]$  concentration (red dots).

### 3.3 Relationship between elasticity coefficient and flux control coefficient

Intuitively, it can be deduced that the rate of an enzyme or group of enzymes or reactions with elasticity coefficients approaching to zero, cannot be increased despite large variations in S (or P) concentration; in consequence, such enzyme(s) exert(s) a high flux control. In turn, an enzyme or group of enzymes with a high elasticity can adjust its/their rate in response to the variation in S or P concentrations, and thus it does not constrain the metabolic flux, implying that it/they exert(s) a low flux control. The relationship between elasticity coefficient and the control of the pathway flux is related through the Connectivity theorem (Fell 1997; Moreno-Sánchez et al 2008b, Saavedra et al 2019).

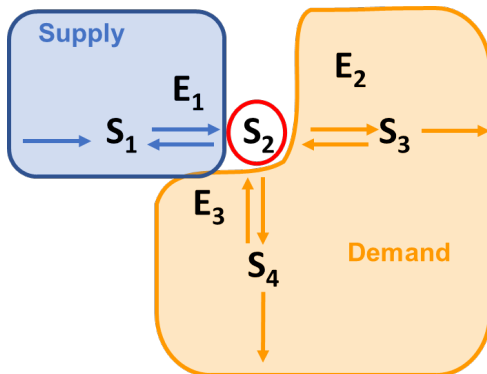
### 3.4 Connectivity theorem

The change in a pathway flux is the result of a concerted response of each of the steps that constitute the pathway. In other words, the system response (the flux) arises from the local responses (elasticities) of the functional units (Kacser 1983). This relationship is reflected in the connectivity theorem, which relates the coefficients of elasticity and control as follows:

$$\sum_{i=1}^n C_{v_i}^J \varepsilon_X^{v_i} = 0 \dots \dots (Eq 12)$$

In practice, two blocks of enzymes (supply and demand) connected by a common metabolite are used for the expression of the connectivity theorem. In scheme 2, a branched pathway is presented along with the expression for its connectivity theorem with respect to metabolite S<sub>2</sub>.

### Scheme 2



$$C_{vE1}^J \varepsilon_{S2}^{vE1} + C_{vE2}^J \varepsilon_{S2}^{vE2} + C_{vE3}^J \varepsilon_{S2}^{vE3} = 0 \quad (Eq\ 13)$$

For unbranched pathways, the summation and connectivity theorems allow the direct calculation of the  $C_{ai}^J$  from the elasticities by solving a system of linear algebraic equations. For systems involving branches and cycles, additional relationships must be used to provide sufficient equations to solve the  $C_{ai}^J$  from the elasticity coefficients (Groen et al 1986; Westerhoff and Kell 1987; Brand 1998).

One of the emblematic studies of elasticity analysis to determine the distribution of flux control was done for gluconeogenesis in rat liver cells where the connectivity and summation theorems were successfully used in order to propose a system of linear algebraic equations for the estimation of the control coefficients for the enzymes of this process (Groen et al 1986). In that study it was demonstrated that pyruvate carboxylase positively and PyK negatively controlled the gluconeogenesis flux in the presence and absence of glucagon, respectively.

Elasticity analysis of the mitochondrial OxPhos indicated that the control is shared between the proton leak and the respiratory chain, being higher for the former (Wanders et al 1984; Hafner et al 1990; Brown et al 1990; Moreno-Sánchez et al 1999). Also, experimental estimation of elasticity coefficients has been done for glycolysis in hepatoma cells where it was determined that the glucose transporter and HK are the most controlling steps (Marín-Hernández et

al 2006). In parasites, elasticity coefficients were used for the determination of the distribution of control of the PPI-dependent glycolysis in *E. histolytica* where the group of reactions of glucose transport/HK/glycogen degradation had a  $C_{ai}^J$  of 0.72-0.86 followed by the bifunctional aldehyde-alcohol dehydrogenase ( $C_{ai}^J$  0.18) (Pineda et al 2015b). Furthermore, it was determined that near 90% inhibition of the low controlling enzyme pyruvate:ferredoxin oxidoreductase ( $C_{ai}^J$  0.13), that is absent in humans, did not significantly decrease the pathway flux. Inhibition of the activity of the steps with the highest control with 2-deoxyglucose and disulfiram decreased the ATP content and cell viability by 60 and 50%, respectively, validating them as drug targets. Again, low control was attained for PPI-PFK ( $C_{ai}^J \leq 0.2$ ).

#### 4. Kinetic modeling for $C_{ai}^J$ determination

Bioinformatics platforms for kinetic modeling of metabolic pathways, such as COPASI (Hoops et al 2006; Bergmann et al 2017) and SCAMP (Sauro 1993), have been successfully applied to determine the flux control distribution of metabolic pathways of parasite and host cells, healthy and pathological cells, and for biotechnologically interesting organisms.

Kinetic modeling requires at least four sets of information (Fig. 8):

1) Kinetic parameters: Kinetic models require thorough kinetic characterization of each enzyme and transporter from the pathway of interest in order to have the parameters (ligand affinity constants,  $V_{max}$ ) that define the rate equation where each effector (inhibitor or activator) must be included and considering the type of reaction mechanism specific for each pathway component (Segel 1975). Several ways to deal with the complexities to define or simplify the rate equations for kinetic modeling have been proposed (Tummler et al 2014; Saa and Nielsen 2017). Many kinetic models are built after mining data of kinetic parameters reported in the literature (Hakenberg et al 2004). Preferably, the kinetic data should all be experimentally determined in the same cell type and under experimental conditions similar to the physiological ones instead of at the optimal pH and temperature of each enzyme (Adamczyk et al 2011; van Eunen et al 2012). For irreversible reactions under physiological conditions, it is useful to use the  $K_{eq}$  of the reaction in the rate equation.

2)  $V_{max}$  in the cell: The actual activity of each enzyme (rate determined under  $V_{max}$  conditions) in the cells or tissue is one of the most important parameters in kinetic models. A close relationship has been found between the  $V_{max}$  value in the cell and the degree of control. Enzymes with low  $V_{max}$  very frequently have high  $C_{ai}^J$ , although an enzyme with high activity in the cell but potent feedback inhibition may also have high control on the flux; however, this cannot be *a priori* inferred from pathway inspection.

3) Concentration of pathway intermediate metabolites. These variables of the system should be best determined in the same cell type and under a specific steady state.

4) Pathway fluxes. The main flux and also the fluxes of the pathway's branches should be determined under the same conditions.

Items one and two are the parameters that serve to build the models in the pathway simulator of choice, whereas items 3 and 4 are the system variables of reference to validate the accuracy of the simulations obtained by the kinetic model built. Usually several iterative rounds of modeling and experimentation are required to obtain a kinetic model that simulates to close proximity the fluxes and pathway intermediates.



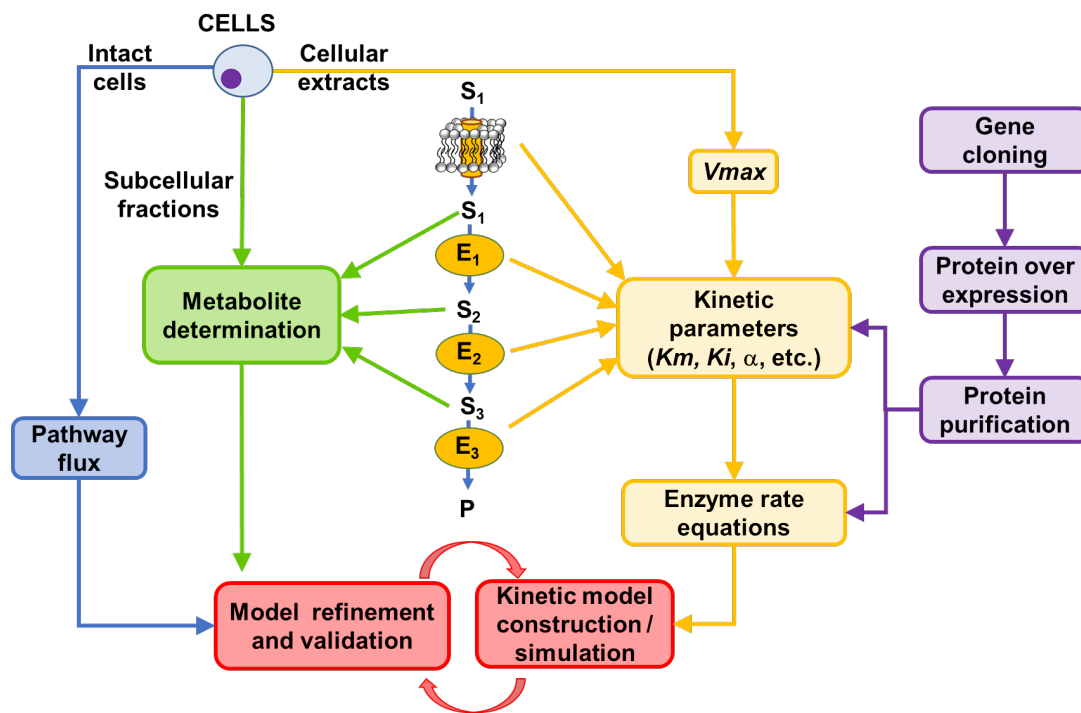


**Figure 8. Requirements for kinetic modeling**

Kinetic modeling requires at least four sets of information, 1) kinetic parameters in rate equations (yellow boxes); 2) the content of active enzyme/transporter ( $V_{max}$ ); 3) concentration of pathway intermediate metabolites (green boxes); 4) pathway fluxes. The kinetic parameters and the rate equations are the main constituents for the construction of the kinetic model of the metabolic pathway using a software for metabolic modeling. The most important kinetic parameter for modeling is  $V_{max}$ , which must be determined in cell extracts or permeabilized cells under the steady-state conditions of interest (initial concentration of substrates, temperature, pH). The other kinetic parameters such as  $K_m$  and  $K_i$ , as well as the rate equations can be determined in cell extracts (yellow boxes) and / or purified recombinant enzymes (purple boxes). Validation of the model predictions is carried out by comparison with the intracellular concentration of metabolites (green boxes) and the total flux of the pathway (blue boxes). It is important to note that there is constant feedback between *in vitro* experimentation and model simulations (circular red arrows), since inconsistencies in the model predictions could mean undescribed interactions that must be investigated to refine the kinetic model.

Kinetic modeling of glycolysis has been used to search for therapeutic targets in *T. brucei* (Bakker et al 1997 and 2000), *E. histolytica* (Saavedra et al 2007; Moreno-Sánchez et al 2008a; Lo-Thong et al 2020), and cancer cells (Marín-Hernández et al 2011 and 2020), for the latter also involving an analysis under hypoxia conditions (Marín-Hernández et al 2014). These studies have shown that, in general, the first part of the pathway constituted by glucose transporter, HK, hexose-6-phosphate isomerase, and glycogen metabolism exerts the greater control ( $\approx 50\%$ ). Furthermore, inhibition of low controlling steps that produce metabolites that inhibit high controlling steps was shown to be a way to arrest glycolysis in cancer cells (Marín-Hernández et al 2016).

The pathways involved in handling oxidative stress have also been studied using kinetic modeling in *T. cruzi* and tumor cells. In the case of *T. cruzi*, two models have been developed, one for the synthesis of trypanothione (Olin-Sandoval et al 2012; González-Chávez et al. 2019) and one for the peroxide detoxification (González-Chávez et al. 2019). The main potential therapeutic targets found in these studies were  $\gamma$ ECS and TryS for trypanothione synthesis, and TXN1 for the peroxide detoxification. In the study by González-Chávez et al. (2019) the  $C_{ai}^J$  obtained by kinetic modeling and genetic manipulation of the enzyme activity (see section 2.4.3) were remarkably similar, mutually validating both methodologies for  $C_{ai}^J$  determination.

In the case of tumor cells, the NADPH supply for oxidative stress handling has been modeled and revealed that peroxide detoxification was mainly controlled by glutathione peroxidase-1 and the cytosolic NADPH supply was mainly controlled by glucose-6-phosphate dehydrogenase (Moreno-Sánchez et al 2017).

Kinetic modeling is useful not only to find potential drug targets, but also to reveal some biochemical aspects that remain unknown or that are unexpected, but which emerge when the interaction among all pathway components is analyzed. For example, the intracellular steady-state concentration of reactive oxygen species (ROS) and even more the ROS concentration in different cellular compartments is very difficult to assess with the currently available techniques. However, it is possible to have a solid approximation by using kinetic models as was illustrated in the studies of

oxidative stress handling in cancer cells (Moreno-Sánchez et al 2017; 2018). Kinetic modeling of OxPhos has also been reported where rather similar  $C_{ai}^J$  values amongst complexes I, III, IV and ATP synthase were found (Heiske et al 2017).

## 5. Conclusion

Metabolic control analysis is a very powerful tool that provides insight into how metabolic pathways work. Understanding the control of metabolic pathways can be used for various purposes, for example basic science, improvement of biotechnological processes, and for drug target selection. From the several examples reviewed in this chapter one can recognize the usefulness and rationality of the approach to identify the best candidates for therapeutic intervention in the metabolism of parasitic and pathological cells. Then, MCA provides an additional strategy in the discovery of new drugs or for repurposing existing drugs by making target selection more efficient. Thus, MCA contributes to reaching the goal of developing therapeutics against diseases afflicting human beings, accelerating the translation of basic science knowledge towards its immediate use and application in humans (translational medicine and science).

## References

1. Adamczyk M, van Eunen K, Bakker BM, Westerhoff HV. Enzyme kinetics for systems biology when, why and how. *Methods Enzymol.* 2011;500:233-57.
2. Albert MA, Haanstra JR, Hannaert V, Van Roy J, Opperdoes FR, Bakker BM, Michels PA. Experimental and in silico analyses of glycolytic flux control in bloodstream form *Trypanosoma brucei*. *J Biol Chem.* 2005. 280(31):28306-15.
3. Bakker BM, Michels PA, Opperdoes FR, Westerhoff HV. Glycolysis in bloodstream form *Trypanosoma brucei* can be understood in terms of the kinetics of the glycolytic enzymes. *J Biol Chem.* 1997; 272(6):3207-15
4. Bakker BM, Westerhoff HV, Opperdoes FR, Michels PA. Metabolic control analysis of glycolysis in trypanosomes as an approach to improve selectivity and effectiveness of drugs. *Mol Biochem Parasitol.* 2000; 106(1):1-10.
5. Bergmann FT, Hoops S, Klahn B, Kummer U, Mendes P, Pahle J, Sahle S. J COPASI and its applications in biotechnology *Biotechnol.* 2017. 261:215-220.
6. Brand MD. Top-down elasticity analysis and its application to energy metabolism in isolated mitochondria and intact cells. *Mol Cell Biochem.* 1998. 184(1-2):13-20.
7. Brown GC, Lakin-Thomas PL, Brand MD. Control of respiration and oxidative phosphorylation in isolated rat liver cells. *Eur J Biochem.* 1990; 192(2):355-62.
8. Castegna A, Gissi R, Menga A, Montopoli M, Favia M, Viola A, Canton M. Pharmacological targets of metabolism in disease: Opportunities from macrophages. *Pharmacol Ther.* 2020; 210:107521
9. Diderich JA, Teusink B, Valkier J, Anjos J, Spencer-Martins I, van Dam K, Walsh MC. Strategies to determine the extent of control exerted by glucose transport on glycolytic flux in the yeast *Saccharomyces bayanus*. *Microbiology (Reading).* 1999. 145 ( Pt 12):3447-3454.
10. De Rycker M, Baragaña B, Duce SL, Gilbert IH. Challenges and recent progress in drug discovery for tropical diseases. *Nature.* 2018. 559(7715):498-506.
11. Fell D. 1997. Understanding the control of metabolism. Portland Press, London. ISBN: 978 1 85578 047 7. ISSN: 1353 6516.
12. Flint HJ, Tateson RW, Barthelmess IB, Porteous DJ, Donachie WD, Kacser H. Control of the flux in the arginine pathway of *Neurospora crassa*. Modulations of enzyme activity and concentration. *Biochem J.* 1981. 15;200(2):231-46.
13. Galluzzi L, Kepp O, Vander Heiden MG, Kroemer G. Metabolic targets for cancer therapy. *Nat Rev Drug Discov.* 2013; 12(11):829-46.
14. Gellerich FN, Kunz WS, Bohnensack R. Estimation of flux control coefficients from inhibitor titrations by non-linear regression. *FEBS Lett.* 1990; 274(1-2):167-70.

15. Giersch C. Determining elasticities from multiple measurements of flux rates and metabolite concentrations. Application of the multiple modulation method to a reconstituted pathway. *Eur J Biochem.* 1995; 227(1-2):194-201.
16. González-Chávez Z, Olin-Sandoval V, Rodríguez-Zavala JS, Moreno-Sánchez R, Saavedra E. Metabolic control analysis of the *Trypanosoma cruzi* peroxide detoxification pathway identifies tryparedoxin as a suitable drug target. *Biochim Biophys Acta.* 2015; 1850(2):263-73
17. González-Chávez Z, Vázquez C, Mejia-Tlachi M, Márquez-Dueñas C, Manning-Cela R, Encalada R, Rodríguez-Enríquez S, Michels PAM, Moreno-Sánchez R, Saavedra E. Gamma-glutamylcysteine synthetase and tryparedoxin 1 exert high control on the antioxidant system in *Trypanosoma cruzi* contributing to drug resistance and infectivity. *Redox Biol.* 2019; 26:101231.
18. González-Chávez Z, Vázquez C, Moreno-Sánchez R, Saavedra E. Metabolic Control Analysis for Drug Target Prioritization in Trypanosomatids. *Methods Mol Biol.* 2020;2116:689-
19. Groen AK, van Roermund CW, Vervoorn RC, Tager JM. Control of gluconeogenesis in rat liver cells. Flux control coefficients of the enzymes in the gluconeogenic pathway in the absence and presence of glucagon. *Biochem J.* 1986. 15;237(2):379-89.
20. Hakenberg J, Schmeier S, Kowald A, Klipp E, Leser U. Finding kinetic parameters using text mining. *OMICS.* 2004. 8(2):131-52.
21. Hafner RP, Brown GC, Brand MD. Analysis of the control of respiration rate, phosphorylation rate, proton leak rate and protonmotive force in isolated mitochondria using the 'top-down' approach of metabolic control theory. *Eur J Biochem.* 1990; 188(2):313-9.
22. Heinrich R, Rapoport TA. A linear steady-state treatment of enzymatic chains. General properties, control and effector strength. *Eur J Biochem.* 1974. 42(1):89-95.
23. Heiske M, Letellier T, Klipp E. Comprehensive mathematical model of oxidative phosphorylation valid for physiological and pathological conditions. *FEBS J.* 2017. 284(17):2802-2828.
24. Hoops S, Sahle S, Gauges R, Lee C, Pahle J, Simus N, Singhal M, Xu L, Mendes P, Kummer U. COPASI--a COmplex PATHway Simulator. *Bioinformatics.* 2006. 22(24):3067-74.
25. Kaambre T, Chekulayev V, Shevchuk I, Tepp K, Timohhina N, Varikmaa M, Bagur R, Klepinin A, Anmann T, Koit A, Kaldma A, Guzun R, Valvere V, Saks V. Metabolic control analysis of respiration in human cancer tissue. *Front Physiol.* 2013. 4:151.
26. Kacser H, Burns JA. The control of flux. *Symp Soc Exp Biol.* 1973. 27:65-104.
27. Kacser H, Burns JA. Molecular democracy: who shares the controls? *Biochem Soc Trans.* 1979. 7(5):1149-60.
28. Kacser H. The control of enzyme systems *in vivo*: Elasticity analysis of the steady state. *Biochem. Soc. Trans.* 1983; 11 (1): 35–40.

29. Kurata M, Yamamoto K, Moriarity BS, Kitagawa M, Largaespada DA. CRISPR/Cas9 library screening for drug target discovery. *J Hum Genet.* 2018. 63(2):179-186.
30. Leroux AE, Krauth-Siegel RL. Thiol redox biology of trypanosomatids and potential targets for chemotherapy. *Mol Biochem Parasitol.* 2016. 206(1-2):67-74.
31. Lo-Thong O, Charton P, Cadet XF, Grondin-Perez B, Saavedra E, Damour C, Cadet F. Identification of flux checkpoints in a metabolic pathway through white-box, grey-box and black-box modeling approaches. *Sci Rep.* 2020. 10(1):13446.
32. Manta B, Bonilla M, Fiestas L, Sturlese M, Salinas G, Bellanda M, Comini MA. Polyamine-Based Thiols in Trypanosomatids: Evolution, Protein Structural Adaptations, and Biological Functions. *Antioxid Redox Signal.* 2018. 28(6):463-486.
33. Marín-Hernández A, Rodríguez-Enríquez S, Vital-González PA, Flores-Rodríguez FL, Macías-Silva M, Sosa-Garrocho M, Moreno-Sánchez R. Determining and understanding the control of glycolysis in fast-growth tumor cells. Flux control by an over-expressed but strongly product-inhibited hexokinase. *FEBS J.* 2006; 273(9):1975-88.
34. Marín-Hernández A, Gallardo-Pérez JC, Ralph SJ, Rodríguez-Enríquez S, Moreno-Sánchez R. HIF-1 $\alpha$  modulates energy metabolism in cancer cells by inducing over-expression of specific glycolytic isoforms. *Mini Rev Med Chem.* 2009. 9(9):1084-101.
35. Marín-Hernández A, Gallardo-Pérez JC, Rodríguez-Enríquez S, Encalada R, Moreno-Sánchez R, Saavedra E. Modeling cancer glycolysis. *Biochim Biophys Acta.* 2011. 1807(6):755-67.
36. Marín-Hernández A, López-Ramírez SY, Del Mazo-Monsalvo I, Gallardo-Pérez JC, Rodríguez-Enríquez S, Moreno-Sánchez R, Saavedra E. Modeling cancer glycolysis under hypoglycemia, and the role played by the differential expression of glycolytic isoforms. *FEBS J.* 2014; 281(15):3325-45.
37. Marín-Hernández Á, Rodríguez-Zavala JS, Del Mazo-Monsalvo I, Rodríguez-Enríquez S, Moreno-Sánchez R, Saavedra E. Inhibition of Non-flux-Controlling Enzymes Deters Cancer Glycolysis by Accumulation of Regulatory Metabolites of Controlling Steps. *Front Physiol.* 2016; 7:412.
38. Marín-Hernández Á, Gallardo-Pérez JC, Reyes-García MA, Sosa-Garrocho M, Macías-Silva M, Rodríguez-Enríquez S, Moreno-Sánchez R, Saavedra E. Kinetic modeling of glucose central metabolism in hepatocytes and hepatoma cells. *Biochim Biophys Acta Gen Subj.* 2020. 1864(11):129687.
39. Michels PAM, Villafraz O, Pineda E, Alencar MB, Cáceres AJ, Silber AM, Bringaud F. Carbohydrate metabolism in trypanosomatids: New insights revealing novel complexity, diversity and species-unique features. *Exp Parasitol.* 2021. 224:108102.
40. Moreno-Sánchez R, Bravo C, Westerhoff HV. Determining and understanding the control of flux. An illustration in submitochondrial particles of how to validate schemes of metabolic control. *Eur J Biochem.* 1999. 264(2):427-33.

41. Moreno-Sánchez R, Encalada R, Marín-Hernández A, Saavedra E. Experimental validation of metabolic pathway modeling. *FEBS J.* 2008a; 275(13):3454-69.
42. Moreno-Sánchez R, Saavedra E, Rodríguez-Enríquez S, Olin-Sandoval V. Metabolic control analysis: a tool for designing strategies to manipulate metabolic pathways. *J Biomed Biotechnol.* 2008b :597913.
43. Moreno-Sánchez R, Saavedra E, Rodríguez-Enríquez S, Gallardo-Pérez JC, Quezada H, Westerhoff HV. Metabolic control analysis indicates a change of strategy in the treatment of cancer. *Mitochondrion.* 2010. 10(6):626-39.
44. Moreno-Sánchez R, Marín-Hernández A, Saavedra E, Pardo JP, Ralph SJ, Rodríguez-Enríquez S. Who controls the ATP supply in cancer cells? Biochemistry lessons to understand cancer energy metabolism. *Int J Biochem Cell Biol.* 2014. 50:10-23
45. Moreno-Sánchez R, Gallardo-Pérez JC, Rodríguez-Enríquez S, Saavedra E, Marín-Hernández Á. Control of the NADPH supply for oxidative stress handling in cancer cells. *Free Radic Biol Med.* 2017. 112:149-161.
46. Moreno-Sánchez R, Marín-Hernández Á, Gallardo-Pérez JC, Vázquez C, Rodríguez-Enríquez S, Saavedra E. Control of the NADPH supply and GSH recycling for oxidative stress management in hepatoma and liver mitochondria. *Biochim Biophys Acta Bioenerg.* 2018. 1859(10):1138-1150.
47. Mukherjee S, Mukherjee N, Gayen P, Roy P, Babu SP. Metabolic Inhibitors as Antiparasitic Drugs: Pharmacological, Biochemical and Molecular Perspectives. *Curr Drug Metab.* 2016; 17(10): 937-970.
48. Müller J, Hemphill A. Drug target identification in protozoan parasites. *Expert Opin Drug Discov.* 2016; 11(8):815-24.
49. Müller M, Mentel M, van Hellemond JJ, Henze K, Woehle C, Gould SB, Yu RY, van der Giezen M, Tielens AG, Martin WF. Biochemistry and evolution of anaerobic energy metabolism in eukaryotes. *Microbiol Mol Biol Rev.* 2012. 76(2):444-95.
50. Nelson, D.L.; Cox, M.M. *Lehninger Principles of Biochemistry.* 7th ed; W.H. Freeman: New York, 2017. Chapter 15.2.
51. Newsholme E. A. and Start C. *Regulation of Metabolism.* John Wiley & Sons, London, UK, 1973.
52. Olin-Sandoval V, Moreno-Sánchez R, Saavedra E. Targeting trypanothione metabolism in trypanosomatid human parasites. *Curr Drug Targets.* 2010. 11(12):1614-30.
53. Olin-Sandoval V, González-Chávez Z, Berzunza-Cruz M, Martínez I, Jasso-Chávez R, Becker I, Espinoza B, Moreno-Sánchez R, Saavedra E. Drug target validation of the trypanothione pathway enzymes through metabolic modelling. *FEBS J.* 2012; 279(10):1811-33.
54. Pineda E., Encalada R., Vázquez C., González Z., Moreno-Sánchez R., Saavedra E. (2015a) Glucose Metabolism and Its Controlling Mechanisms in

- Entamoeba histolytica*. In: Nozaki T., Bhattacharya A. (eds) Amebiasis. Springer, Tokyo.
55. Pineda E, Encalada R, Vázquez C, Néquiz M, Olivos-García A, Moreno-Sánchez R, Saavedra E (2015b). In vivo identification of the steps that control energy metabolism and survival of *Entamoeba histolytica*. FEBS 282(2):318-31
  56. Piñeyro MD, Arias D, Parodi-Talice A, Guerrero S, Robello C. Trypanothione Metabolism as Drug Target for Trypanosomatids. Curr Pharm Des. 2021. 27(15):1834-1846.
  57. Raj S, Sasidharan S, Balaji SN, Saudagar P. An overview of biochemically characterized drug targets in metabolic pathways of Leishmania parasite. Parasitol. Res. 2020; 119(7): 2025-2037.
  58. Rodríguez-Enríquez S, Torres-Márquez ME, Moreno-Sánchez R. Substrate oxidation and ATP supply in AS-30D hepatoma cells. Arch Biochem Biophys. 2000; 375(1):21-30.
  59. Saavedra E, Marín-Hernández A, Encalada R, Olivos A, Mendoza-Hernández G, Moreno-Sánchez R. Kinetic modeling can describe in vivo glycolysis in *Entamoeba histolytica*. FEBS J. 2007; 274(18):4922-40.
  60. Saavedra E, González-Chávez Z, Moreno-Sánchez R, Michels PAM. Drug Target Selection for *Trypanosoma cruzi* Metabolism by Metabolic Control Analysis and Kinetic Modeling. Curr Med Chem. 2019. 26(36):6652-6671.
  61. Saavedra E, Encalada R, Vázquez C, Olivos-García A, Michels PAM, Moreno-Sánchez R. Control and regulation of the pyrophosphate-dependent glucose metabolism in *Entamoeba histolytica*. Mol Biochem Parasitol. 2019. 229:75-87.
  62. Saa PA, Nielsen LK. Formulation, construction and analysis of kinetic models of metabolism: A review of modelling frameworks. Biotechnol Adv. 2017. 35(8):981-1003.
  63. Sauro HM. SCAMP: a general-purpose simulator and metabolic control analysis program. Comput Appl Biosci. 1993. 9(4):441-50.
  64. Segel I.H. 1975. Enzyme Kinetics. Wiley, New York, USA
  65. Schuster A, Erasimus H, Fritah S, Nazarov PV, van Dyck E, Niclou SP, Golebiewska. A RNAi/CRISPR Screens: from a Pool to a Valid Hit. Trends Biotechnol. 2019. 37(1):38-55.
  66. Small JR, Kacser H. Responses of metabolic systems to large changes in enzyme activities and effectors. 1. The linear treatment of unbranched chains. Eur J Biochem. 1993a. 213(1):613-24.
  67. Small JR, Kacser H. Responses of metabolic systems to large changes in enzyme activities and effectors. 2. The linear treatment of branched pathways and metabolite concentrations. Assessment of the general non-linear case. Eur J Biochem. 1993b. 213(1):625-40.
  68. Soares Medeiros LC, South L, Peng D, Bustamante JM, Wang W, Bunkofske M, Perumal N, Sanchez-Valdez F, Tarleton RL. Rapid, Selection-Free, High-



- Efficiency Genome Editing in Protozoan Parasites Using CRISPR-Cas9 Ribonucleoproteins. *mBio*. 2017. 8(6):e01788-17.
69. Sukjoi W, Ngamkham J, Attwood PV, Jitrapakdee S. Targeting Cancer Metabolism and Current Anti-Cancer Drugs. *Adv Exp Med Biol*. 2021. 1286:15-48.
70. Talevi A, Carrillo C, Comini M. The Thiol-polyamine Metabolism of *Trypanosoma cruzi*: Molecular Targets and Drug Repurposing Strategies. *Curr Med Chem*. 2019. 26(36):6614-6635.
71. Torres NV, Mateo F, Meléndez-Hevia E, Kacser H. Kinetics of metabolic pathways. A system in vitro to study the control of flux. *Biochem J*. 1986. 234(1):169-74.
72. Torres NV, Souto R, Meléndez-Hevia E. Study of the flux and transition time control coefficient profiles in a metabolic system in vitro and the effect of an external stimulator. *Biochem J*. 1989. 260(3):763-9.
73. Tummler, K.; Lubitz, T.; Schelker, M.; Klipp, E. New types of experimental data shape the use of enzyme kinetics for dynamic network modeling. *FEBS J.*, 2014, 281(2), 549-571.
74. Tyagi R, Elfawal MA, Wildman SA, Helander J, Bulman CA, Sakanari J, Rosa BA, Brindley PJ, Janetka JW, Aroian RV, Mitreva M. Identification of small molecule enzyme inhibitors as broad-spectrum anthelmintics. *Sci Rep*. 2019. 9(1):9085.
75. Valente M, Vidal AE, González-Pacanowska D. Targeting Kinetoplastid and Apicomplexan Thymidylate Biosynthesis as an Antiprotozoal Strategy. *Curr Med Chem*. 2019. 26(22):4262-4279.
76. van Eunen K, Kiewiet JA, Westerhoff HV, Bakker BM. Testing biochemistry revisited: how in vivo metabolism can be understood from in vitro enzyme kinetics. *PLoS Comput Biol*. 2012;8(4):e1002483.
77. Wanders RJ, Groen AK, Van Roermund CW, Tager JM. Factors determining the relative contribution of the adenine-nucleotide translocator and the ADP-regenerating system to the control of oxidative phosphorylation in isolated rat-liver mitochondria. *Eur J Biochem*. 1984. 142(2):417-24.
78. Westerhoff HV, Kell DB. Matrix method for determining steps most rate-limiting to metabolic fluxes in biotechnological processes. *Biotechnol Bioeng*. 1987. 30(1):101-7.
79. Wyatt PG, Gilbert IH, Read KD, Fairlamb AH. Target validation: Linking target and chemical properties to desired product profile. *Curr. Top. Med. Chem*. 2011. 11:1275–1283.